Low temperature incorporation of selenium in Cu_2ZnSnS_4: Diffusion and nucleation

Sigbjørn Grini*[1], Nils Ross[1,2], Clas Persson[1], Charlotte Platzer-Björkman[2] and Lasse Vines[1]

[1]Department of Physics, Center for Materials Science and Nanotechnology, University of Oslo, P.O.Box 1048, Blindern, N-0316 Oslo, Norway

[2]Ångström Solar Center, Division of Solid State Electronics, Uppsala University, Uppsala, Uppland, 75120, Sweden

*Corresponding author: sigbjorn.grini@smn.uio.no, Phone: +47 470 91 335, Fax: +47 22 85 64 22

ABSTRACT

Band gap grading of $Cu_2ZnSn(S,Se)_4$ (CZTSSe) solar cells can be achieved by varying the S_r = [S]/([S] + [Se]) ratio in the absorber layer with depth. One approach is a two-step annealing process where the absorber is first sulfurized to Cu_2ZnSnS_4 (CZTS) followed by selenization to form CZTSSe. However, once nucleation of CZTSSe initiates, the rapid interchange of S and Se limits the control over the S_r ratio with depth. Here, we have studied incorporation of Se into CZTS and observed the behavior of Se below and up to the nucleation temperature of CZTSSe. Se diffusion at 337 and 360 °C is dominated by grain boundary diffusion while some increase of Se is also seen in the region from 100 to 800 nm from the surface. After selenization at 409 °C, recrystallization is observed and CZTSSe grains are formed. The recrystallization is more rapid for a smaller average grain size and is facilitated by diffusion of Na from the back contact. The grain boundary diffusion is identified with secondary ion mass spectrometry measurements by measuring the accumulation in the CZTS/Mo interface for three samples with different average grain size.

Keywords: Cu_2ZnSnS_4; selenium diffusion; band gap grading; nucleation; recrystallization; grain boundary diffusion; diffusion; secondary ion mass spectrometry

1 INTRODUCTION

The best $Cu_2ZnSn(S,Se)_4$ (CZTSSe) devices produced to date have introduced the chalcogens S and Se either as part of the precursor or as gas during the crystallization process [1–5]. By including both chalcogens in the complex crystallization process, control of their diffusion and nucleation is limited, and it is difficult to obtain a controlled S_r = [S]/([S] + [Se]) ratio with depth. Nevertheless, there are pathways to achieve an S_r gradient in the CZTSSe layer by having S and Se annealed in two steps or through non-symmetric annealing conditions [2,6–8]. If the anneals are performed at low crystallization temperatures, partial recrystallization of the absorber may occur which results in a lateral non-homogeneous distribution of S and Se [9], which can falsely be interpreted as an S_r gradient with grazing incident X-ray diffraction (GIXRD) or conventional secondary ion mass spectrometry (SIMS) depth profile [10]. Previously, we have discussed the practical limitations of chalcogen control in the crystallization process, where sodium assists grain growth [11]. To achieve a controlled S_r gradient a possible approach is to complete a full crystallization with either S or Se and subsequently diffuse in the other chalcogen without triggering nucleation. The challenge is that the energy required to diffuse Se into the existing grains is similar or perhaps higher than the energy required to start to nuclear new grains. In this work we evaluate the diffusion of Se into CZTS at temperatures up to nucleation by annealing in a selenium ambient at 337, 360 and 409 °C for three samples with different average grain size.

2 EXPERIMENTAL DETAILS

Bilayer molybdenum back contact was sputtered onto a soda-lime glass substrate. Cu_2ZnSnS_4 precursors were co-sputtered using CuS, ZnS and SnS targets in a Lesker CMS-18 sputter system. Elemental compositions in the precursors were determined with Rutherford backscattering calibrated X-ray fluorescence (XRF) measurements. The samples were sulfurized into Cu_2ZnSnS_4 for 10, 20 and 40 minutes at 500 ± 10 °C in a tube furnace within a pyrolytic carbon coated graphite box with 80 mg of elemental sulfur placed in a small hole on each side of the box and an argon pressure in the furnace of 35 kPa. The temperature was chosen to avoid secondary phase formation and loss of sulfur as have previously shown to occur at higher temperatures for our furnace [12]. After sulfurization and initial characterization, each sample was subjected to an anneal in the same tube furnace with 90 mg Se in the graphite box and an argon pressure of 35 kPa at 337 ± 10, 360 ± 10 and 409 ± 10 °C for 30 minutes, from now on called "selenization". The cation ratios and sulfurization conditions are described in Table 1.

A Bruker AXS D8 Discover X-ray diffraction (XRD) system was used to study structural properties of the samples before and after selenization. Each sample was surveyed with a θ/2θ scan ranging from 10° to 65° with an increment of 0.01° and a high-resolution scan from 27° to 29° with an increment of 0.002° to study the (112) reflection in detail. Cross-sectional scanning electron microscopy (SEM) images were obtained using a Zeiss Leo 1550 with a 5 kV accelerating voltage. Top-view SEM images were obtained with JEOL

JSM-IT300 with a 5 kV accelerating voltage. The samples were studied with secondary ion mass spectrometry (SIMS) using a Cameca IMS 7f magnetic sector instrument. 5 keV Cs^+ primary ions were mainly used, and the beam was rastered over an area of 150 × 150 μm^2 with a current of 20 nA. Secondary MCs^+ cluster ions were detected from the central part of the crater (33 µm in diameter), where "M" is the element of interest. The ionization of MCs^+ cluster ions is suggested to be less influenced by a change in concentration of matrix elements compared to that of M^+ ions since the Cs^+ ions are previously ionized as the primary beam [13]. The cluster $^{80}Se\,^{133}Cs$ was considered most suited to observe Se given its abundance and $^{23}Na^{133}Cs$ was used to track Na. Control measurements were also carried out on selected samples by detecting negative ions with a 15 keV Cs^+ primary beam and positive ions with 10 keV O_2^+ primary beam to confirm that no significant interference occurred. The sputter time was converted to depth by measuring the depth of the crater with a Stylus profilometer. For measurements on the same sample after heat treatment the depth was calibrated with the inflection point of the $^{98}Mo^{133}Cs$ signal at the interface between CZTS and Mo. An overview over the experiment is displayed in Fig. 1.

Table 1. Cation ratios measured with X-ray fluorescence of the precursor and sulfurization conditions in the tube furnace.

Sample name	**Cation ratios**		**Sulfurization conditions**	
	[Cu]/[Sn]	[Zn]/([Cu]+[Sn])	Temperature (°C)	Time (minutes)
A	1.92 ± 0.02	0.35 ± 0.02	500 ± 10	10
B	1.92 ± 0.02	0.35 ± 0.02	500 ± 10	20
C	1.92 ± 0.02	0.35 ± 0.02	500 ± 10	40

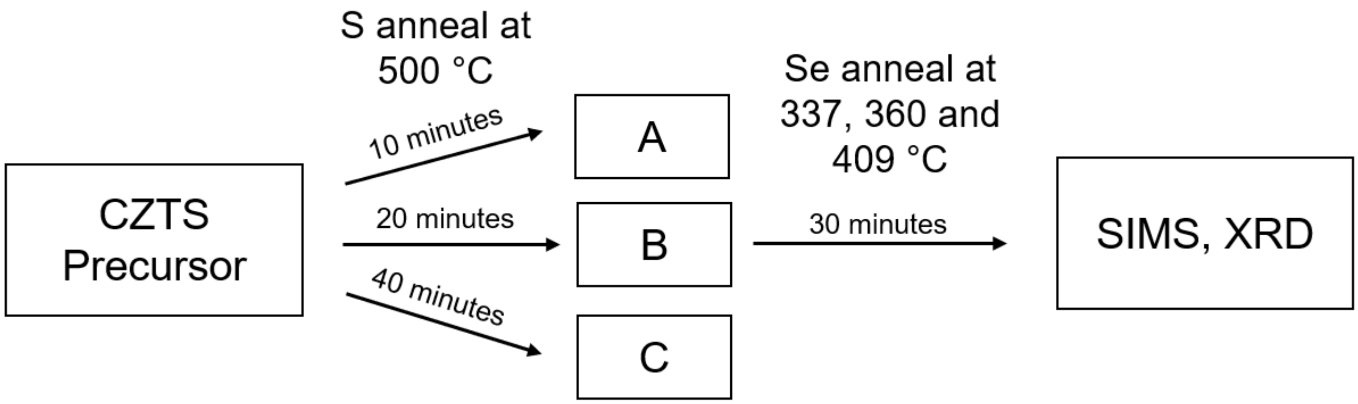

Figure 1. Overview over the experiment. CZTS precursors were sulfurized at 500 °C for 10, 20 and 40 minutes and produced samples A, B and C respectively. Each sample was subsequently selenized at 337, 360 and 409 °C and characterized with secondary ion mass spectrometry (SIMS) and X-ray diffraction (XRD).

3 RESULTS AND DISCUSSION

Figure 2 displays cross sectional SEM images of the samples A, B and C which was sulfurized at 10, 20 and 40 minutes at 500 °C, respectively. The images show a ~1 μm CZTS layer on top of a Mo back contact, in addition to secondary phase formation of SnS_2 (in sample B). However, the amount of secondary phase formation was sufficiently low, so that it did not interfere with subsequent measurements. The variation in sulfurization time results in different average grain sizes as previously demonstrated with the same furnace and sputtering system, and where the average grain size, R, is dependent on annealing time, t, with $R \propto t^{1/n}$ where n is between 2.2 and 2.4 [12]. The average grain size was estimated by counting the number of grain boundaries over a line drawn across the image and divided by its length, as shown in Fig. 3, where the extracted average and variation in grain size, in addition to the estimate with $R \propto t^{1/2.3}$, are displayed. Indeed, Fig. 3 demonstrates that the average grain size increases with approximately 50 % from the sample annealed for 10 minutes compared to that annealed for 40 minutes. Thus, one can expect that the influence of grain boundary diffusion is different for different sulfurization times.

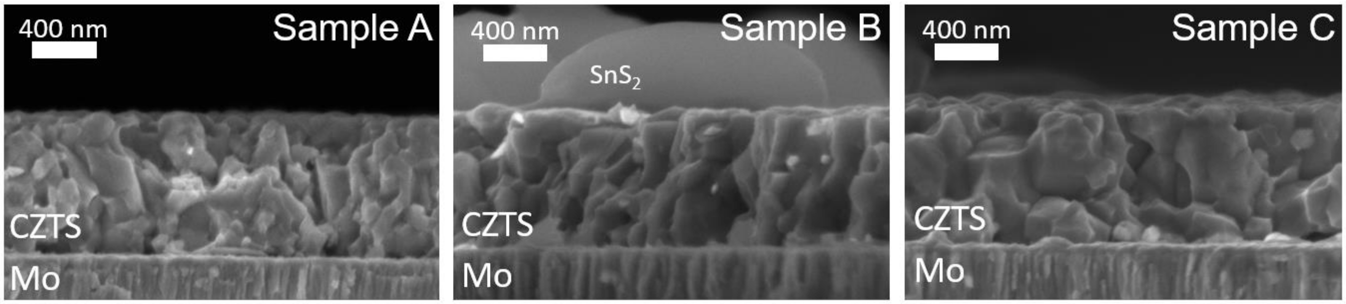

Figure 2. Cross-sectional scanning electron microscopy (SEM) images of the CZTS samples A, B and C which was sulfurized at 500 °C for 10, 20 and 40 minutes respectively from the same precursor. Some SnS2 is observed on the SEM image of sample B but was also seen on top of all samples with an optical microscope.

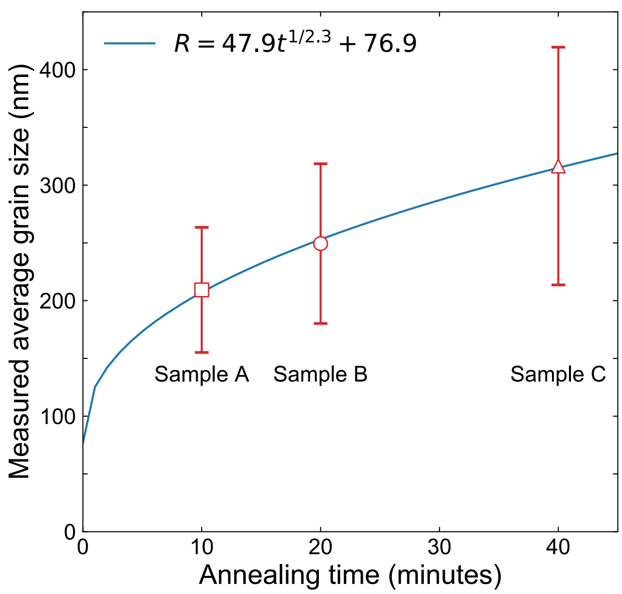

Figure 3. Extracted average grain size, R, (red markers) and the variation (red bars), as a function of annealing temperature for the samples A, B and C which was sulfurized at 500 °C for 10, 20 and 40 minutes respectively from the same precursor. R was estimated using top view SEM images (not shown). 5 horizontal and 5 vertical equally spaced lines were drawn for two images for each sample. The blue line illustrates fitting equation for $R \propto t^{(1/2.3)}$, adapted from Ren et al. [12], and the parameters are shown in the legend.

Figure 4 shows the $^{80}Se^{133}Cs$ signals measured with SIMS for sample B after selenizations at 337, 360 and 409 °C for 30 minutes. Similar temperature dependencies are observed for samples A and C. The background signal (solid gray line) was obtained prior to the Se heat treatments. Selenization at 337 °C resulted in a considerable increase of Se signal at the CZTS/Mo interface, and a minor increase in the region between 100 and 800 nm from the surface, hereafter called “bulk”. The Se content close to the surface is about 2.5 times higher than that in the bulk, e.g. (Fig. 4), indicating that the surface acts as a source for the Se, as expected. However, after selenization at 360 °C, the bulk Se signal is unchanged. This may indicate that the grain boundaries become saturated with Se at 337 °C. Hence, migration of Se may still occur, but the concentration will not increase further. This is substantiated by an increase in Se at the CZTS/Mo interface of a factor 2. After selenization at 409 °C, the Se signal has increased by around one order of magnitude in the bulk and the signal is increasing with depth. The increase in Se correlates with a significant decrease in the S signal (not shown).

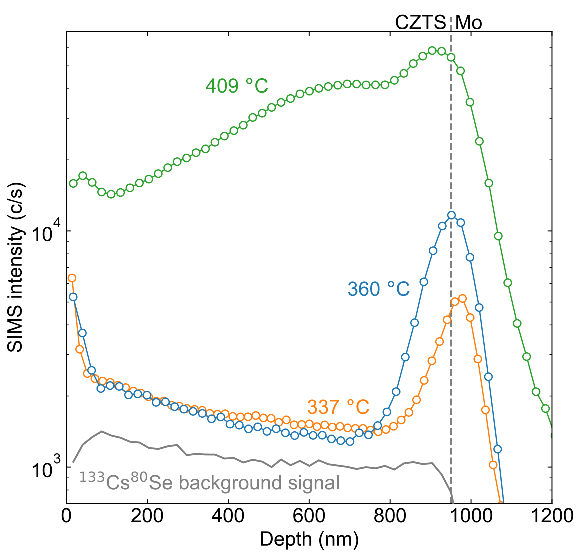

Figure 4: Secondary ion mass spectrometry (SIMS) 80Se133Cs signals for sample B which was sulfurized at 500 °C for 20 minutes followed by selenization at 337 (orange circles), 360 (blue circles) and 409 °C (green circles) for 30 minutes. Se accumulates at the back contact after selenization at 337 °C and the accumulation is greater after selenization at 360 °C. After selenization at 409 °C Se has heavily been incorporated into the CZTS layer and the signal has increased by around one order of magnitude.

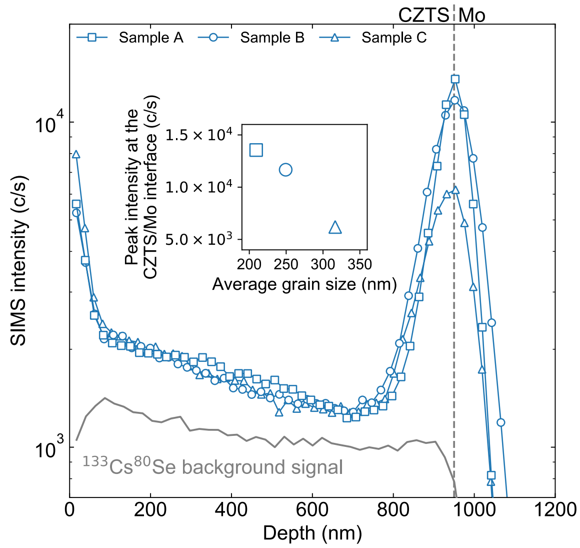

Figure 5. Secondary ion mass spectrometry (SIMS) 80Se133Cs signals for samples A (squares), B (circles) and C (triangles) which was sulfurized at 500 °C for 10, 20 and 40 minutes respectively from the same precursor followed by selenization at 360 °C for 30 minutes. Se accumulates at the CZTS/Mo interface for all samples which inversely correlate with average grain size and solidifies that Se diffuses through grain boundaries at 360 °C. Inset: Peak intensity at the CZTS/Mo interface from each SIMS depth profile versus the average grain size, R, estimated from top-view SEM images.

The Se signals for all three samples after selenization at 360 °C for 30 minutes are displayed in Fig. 5. The figure shows that the sample with the largest average grain size, i.e. sample C, displays a lower Se signal at the CZTS/Mo interface compared to that of samples A and B. Hence, the Se accumulation at the CZTS/Mo interface inversely correlates with grain size and corroborates that the accumulation is promoted by grain boundary diffusion. The inset displays the relationship between the maximum intensity of Se at the CZTS/Mo interface and the estimated average grain size. Figure 6 shows X-ray diffraction (XRD) patterns of high resolution θ/2θ scans from 27° to 29° with an increment of 0.002° for the three samples as-deposited, after selenizations at 360 and 409 °C for 30 minutes. The peaks at 27.48° correlate with the (112) reflection of $Cu_2ZnSn(S_x,Se_{1-x})_4$ (CZTSSe) where x ≈ 0.25 [6] and the peaks 28.49° correlate with the (112) reflection of sulfide Cu_2ZnSnS_4. All samples, as-deposited as well as after a selenization at 360 °C, have a strong signal at the sulfide CZTS position and no signal attributed to CZTSSe. After the selenization at 409

°C the sulfide CZTS signal is reduced and a CZTSSe peak has appeared, indicating that two separate phases occur. The recrystallization process is likely to be inhomogeneous with depth which explains why the Se signal after selenization at 409 °C from Fig. 4 may indicate the presence of a gradient as previously observed using similar annealing conditions [9].

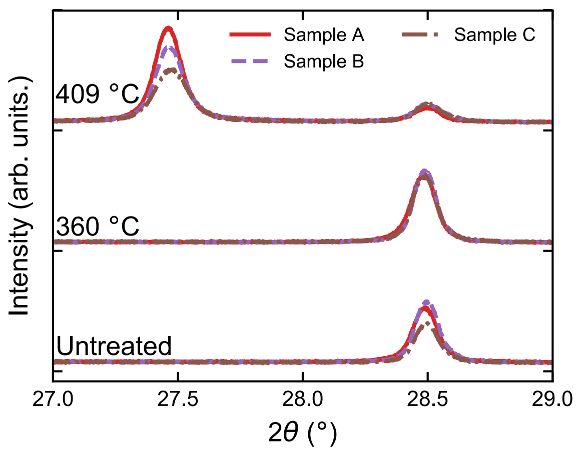

Figure 6. X-ray diffraction (XRD) θ/2θ high resolution scan from 27° to 29° with an increment of 0.002° for three Cu2ZnSnS4 samples (A, B and C) which was sulfurized at 500 °C for 10, 20 and 40 minutes respectively from the same precursor. The patterns show as-deposited and after selenizations at 360 and 409 °C for each sample. The peaks at 28.49° correlates with the (112) reflection of a pure sulfide Cu2ZnSnS4. After the 409 °C anneal, a peak at 27.48° appears for all samples which correlates with the (112) reflection of a new phase Cu2ZnSn(Sx,Se1-x)4 where x ≈ 0.25 [6].

Figure 7 shows the normalized $^{23}Na^{133}Cs$ signals (closed markers) from SIMS for samples A, B and C after selenizations at 360 °C (blue) and 409 °C (green). The $^{80}Se^{133}Cs$ signal after selenization at 409 °C is shown as open markers. Like the behavior of Se after the selenization at 409 °C in sample B (Fig. 5), sample A and C shows a plateau in the Se concentration at around 4×10^4 counts/s, and extending ~550, ~400, and ~300 nm towards the surface for sample A, B and C, respectively. This is in good agreement with the formation of a CZTSSe phase observed by XRD (Fig. 6), indicating that the CZTSSe is formed close to the Mo back contact. This contrasts with reports on CZTSSe formation at higher temperatures where recrystallization has occurred towards the front [11,14]. Since recrystallization is initiated close to the Mo back contact after selenization at 409 °C, this suggests that the grain boundary diffusion and agglomeration at the back contact is an important vehicle for the CZTSSe formation at reduced temperatures. For the behavior of Na, in both the as-deposited (not shown) and the selenization at 360 °C, Na is found at and around the CZTS/Mo interface, with some Na diffused into the CZTS layer. However, at 409 °C, the peak intensity of the Na signal shifts from the CZTS/Mo interface and 150-200 nm into the bulk of the CZTS for all samples. Interestingly, the position of this peak aligns with a local step in the Se signal. Moreover, the peak intensity of the Na signal after selenization at 409 °C increases from sample A to C, i.e. increases with grain size, and hence inversely proportional to the Se concentration observed by SIMS and CZTSSe phase as observed by XRD (Fig. 6). Since both Se and Na are expected to migrate in the grain boundaries it points toward that there is a limited amount of grain boundary sites for Se and Na to occupy, and where Se appear to replace Na in the grain boundaries at this temperature. Here it should be noted that the samples are quenched by being transferred quickly out of the hot zone to the cold zone which suggests that the observed Na accumulation represents the situation at the end of the anneal.

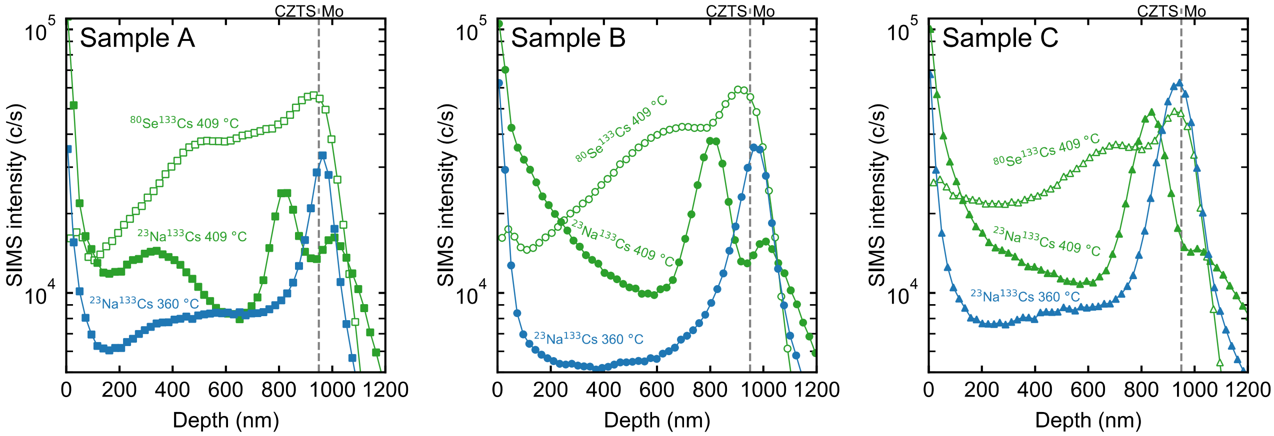

Figure 7. Secondary ion mass spectrometry (SIMS) 23Na133Cs signals (closed markers) for samples A, B and C which was sulfurized at 500 °C for 10, 20 and 40 minutes respectively from the same precursor followed by a selenization at 360 °C (blue) and 409 °C (green) for 30 minutes. The 80Se133Cs signals after the Se anneal at 409 °C is displayed as green open markers. The peak intensity has shifted from the Mo layer close to the CZTS/Mo interface to more inside the CZTS layer where Se has a local step.

In previous studies it has been reported that Na is mainly found in the grain boundaries in CZTS [14] and that Na diffuses more easily in the grain boundaries for $Cu(In,Ga)Se_2$ (CIGS) [15]. If the vast transportation of Na from the back contact into the CZTS layer displayed in Fig. 7 for all samples has transpired through the grain boundaries and into new grains (likely via liquid Na_2Se_x [16]), this would suggest a substantially higher flux of atoms in the grain boundaries at 409 °C compared to the situation at 360 °C. Consequently, the diffusivity of Se increases and Se is easily transported throughout the absorber which means that the recrystallization is not limited by the availability of Se, but rather by the most energetically favorable location where Na is present in sufficient amounts. This would explain the increased Se signal towards the Mo back contact during recrystallization where more recrystallization has occurred closer to the source of Na. However, this behavior is different to previous studies where sulfurized absorbers have been selenized at 425 °C and 450 °C, and where Se have formed grains also towards the front of the absorber [10,11]. We believe the higher temperature annealing condition has caused more favorable recrystallization conditions towards the front which is also accompanied by quick Na diffusion from the back contact. Importantly, for all selenized CZTS absorbers we observe a correlation between increased Na signal and increased Se signal. A suggestion for further work is to diffuse Se into Na-free CZTS to observe the effect of not having Na present on Se diffusion and nucleation. Additionally, low temperature diffusion of S into selenide $Cu_2ZnSnSe_4$ (CZTSe) absorbers should be investigated further [17].

4 CONCLUSIONS

In this paper we demonstrate that Se diffuses into sulfide CZTS grain boundaries during selenization at 337 and 360 °C for 30 minutes. While some increased signal of Se is observed in the bulk region from 100 to 800 nm from the surface, the diffusion can be explained by an increased concentration of Se in the grain boundaries. Once the samples are subjected to a selenization at 409 °C for 30 minutes, nucleation of CZTSSe causes recrystallization of CZTSSe grains and a great increase of Se signal from SIMS is observed in the CZTS layer. The recrystallization dominates the incorporation of Se into CZTS and suppresses the possible in-diffusion into grains to form a band gap gradient. At sufficient temperatures Na diffuses from the back contact and into the CZTS layer, facilitates the recrystallization and enhances Se grain boundary diffusion. These results show that a controlled diffusion of Se in sulfide CZTS grains to form a band gap gradient is not feasible suggesting that the energy required to recrystallize new CZTSSe grains is lower compared to diffusion into existing grains. While this conclusion should be valid for most systems, the recrystallization could potentially be suppressed by controlling the Na incorporation or by low temperature incorporation of S into CZTSe grains.

ACKNOWLEDGEMENTS

This work has been funded by the Research Council of Norway (project 243642) and the Swedish Foundation for Strategic Research. The Research Council of Norway is also acknowledged for the support to the Norwegian Micro and Nano-Fabrication Facility, NorFab, project number 245963/F50. S. G. would like to thank G. C. Vasquez for assistance with SEM top-view measurements.

REFERENCES

[1] T.K. Todorov, J. Tang, S. Bag, O. Gunawan, T. Gokmen, Y. Zhu, D.B. Mitzi, Beyond 11% efficiency: Characteristics of state-of-the-art $Cu_2ZnSn(S,Se)_4$ Solar Cells, Adv. Energy Mater. 3 (2013) 34–38.

[2] S. Wu, C. Chang, H. Chen, C. Shih, Y. Wang, C. Li, S. Chan, High-efficiency $Cu_2ZnSn(S,Se)_4$ solar cells fabricated through a low-cost solution process and a two-step heat treatment, Prog. Photovoltaics Res. Appl. 25 (2017) 58–66.

[3] J.K. Larsen, Y. Ren, N. Ross, E. Särhammar, S.-Y. Li, C. Platzer-Björkman, Surface modification through air annealing $Cu_2ZnSn(S,Se)_4$ absorbers, Thin Solid Films. 633 (2017) 118–121.

[4] D.-K. Hwang, B.-S. Ko, D.-H. Jeon, J.-K. Kang, S.-J. Sung, K.-J. Yang, D. Nam, S. Cho, H. Cheong, D.-H. Kim, Single-step sulfo-selenization method for achieving low open circuit voltage deficit with band gap front-graded $Cu_2ZnSn(S,Se)_4$ thin films, Sol. Energy Mater. Sol. Cells. 161 (2017) 162–169.

[5] S.G. Haass, M. Diethelm, M. Werner, B. Bissig, Y.E. Romanyuk, A.N. Tiwari, 11.2% Efficient Solution Processed Kesterite Solar Cell with a Low Voltage Deficit, Adv. Energy Mater. 5 (2015) 1–7.

[6] P.M.P. Salomé, J. Malaquias, P.A. Fernandes, M.S. Ferreira, A.F. da Cunha, J.P. Leitão, J.C. González, F.M. Matinaga, Growth and characterization of $Cu_2ZnSn(S,Se)_4$ thin films for solar cells, Sol. Energy Mater. Sol. Cells. 101 (2012) 147–153.

[7] K.-J. Yang, D.-H. Son, S.-J. Sung, J.-H. Sim, Y.-I. Kim, S.-N. Park, D.-H. Jeon, J. Kim, D.-K. Hwang, C.-W. Jeon, D. Nam, H. Cheong, J.-K. Kang, D.-H. Kim, A band-gap-graded CZTSSe solar cell with 12.3% efficiency, J. Mater. Chem. A. 4 (2016) 10151–10158.

[8] K. Woo, Y. Kim, W. Yang, K. Kim, I. Kim, Y. Oh, J.Y. Kim, J. Moon, Band-gap-graded $Cu_2ZnSn(S_{1-x},Se_x)_4$ solar cells fabricated by an ethanol-based, particulate precursor ink route., Sci. Rep. 3 (2013) 3069.

[9] N. Ross, J. Larsen, S. Grini, E. Särhammar, L. Vines, C. Platzer Björkman, $Cu_2ZnSn(S,Se)_4$ Solar Cell Absorbers from Diffusion of Selenium into Annealed CZTS Absorbers, Procedings 2016 IEEE 43th Photovolt. Spec. Conf. (2016) 492–497.

[10] S. Grini, N. Ross, T.N. Sky, C. Persson, C. Platzer-Björkman, L. Vines, Secondary ion mass spectrometry as a tool to study selenium gradient in $Cu_2ZnSn(S,Se)_4$, Phys. Status Solidi C 14 (2017) 1600187.

[11] N. Ross, J. Larsen, S. Grini, L. Vines, C. Platzer-Björkman, Practical limitations to selenium annealing of compound co-sputtered Cu_2ZnSnS_4 as a route to achieving sulfur-selenium graded solar cell absorbers, Thin Solid Films. 623 (2017) 110–115.

[12] Y. Ren, N. Ross, J.K. Larsen, K. Rudisch, J.J.S. Scragg, C. Platzer-Björkman, Evolution of Cu_2ZnSnS_4 during Non-Equilibrium Annealing with Quasi-in Situ Monitoring of Sulfur Partial Pressure, Chem. Mater. 29 (2017) 3713–3722.

[13] C.W. Magee, W.L. Harrington, E.M. Botnick, On the use of CsX+ cluster ions for major element depth profiling in secondary ion mass spectrometry, Int. J. Mass Spectrom. Ion Process. 103 (1990) 45–56.

[14] S. Tajima, R. Asahi, D. Isheim, D.N. Seidman, T. Itoh, K.I. Ohishi, Sodium distribution in solar-grade Cu2ZnSnS4 layers using atom-probe tomographic technique, Jpn. J. Appl. Phys. 54 (2015) 11.

[15] A. Laemmle, R. Wuerz, T. Schwarz, O. Cojocaru-Mirédin, P.-P. Choi, M. Powalla, Investigation of the diffusion behavior of sodium in $Cu(In,Ga)Se_2$ layers, J. Appl. Phys. 115 (2014) 154501.

[16] C.M. Sutter-Fella, J. a. Stückelberger, H. Hagendorfer, F. La Mattina, L. Kranz, S. Nishiwaki, A.R. Uhl, Y.E. Romanyuk, A.N. Tiwari, Sodium Assisted Sintering of Chalcogenides and Its Application to Solution Processed $Cu_2ZnSn(S,Se)_4$ Thin Film Solar Cells, Chem. Mater. 26 (2014) 1420–1425.

[17] S.P. Harvey, I. Repins, G. Teeter, Defect chemistry and chalcogen diffusion in thin-film $Cu_2ZnSnSe_4$ materials, J. Appl. Phys. 117 (2015) 074902.